AJNR

Tumors of the nasopharynx and adjacent areas: MR imaging with Gd-DTPA.

T Vogl, S Dresel, L T Bilaniuk, G Grevers, K Kang and J Lissner

AJNR Am J Neuroradiol 1990, 11 (1) 187-194
http://www.ajnr.org/content/11/1/187

Tumors of the Nasopharynx and Adjacent Areas: MR Imaging with Gd-DTPA

T. Vogl[1]
S. Dresel[1]
L. T. Bilaniuk[2]
G. Grevers[3]
K. Kang[1]
J. Lissner[1]

The purpose of this study was to describe our experience with Gd-DTPA–enhanced MR imaging in the evaluation of the most common nasopharyngeal tumors. Forty-two patients with tumors of the nasopharynx and adjacent spaces had MR imaging before and after IV injection of Gd-DTPA. Images were obtained with a 1.0-T superconducting magnet imaging system in transverse, coronal, and sagittal planes with T1- and T2-weighted sequences. MR images were compared with CT scans and tumor histology. The studies were categorized by using a grading system with grades ranging from unsatisfactory (grade 0) to optimal (grade 3). Contrast-enhanced MR enables better identification of small anatomic details such as both palatini muscles and the pharyngobasilar fascia. MR after Gd-DTPA was superior to CT in all cases except for tumors of the maxillary sinuses.

MR with Gd-DTPA is recommended for tumors that are small and difficult to detect on the initial nonenhanced MR examination or that show subtle infiltrations. Because of the increased cost and longer examination time, MR with Gd-DTPA does not need to be done when large tumors are well delineated.

AJNR 11:187–194, January/February 1990; *AJR* 154: March 1990

The complex patterns created by spread of nasopharyngeal tumors with involvement of soft tissue and bony structures require an imaging method that distinguishes both soft tissue and bone. MR imaging has shown that its superior soft-tissue contrast resolution depicts tumor margins in the nasopharynx and related spaces more accurately than CT does [1–3]. Thus, MR has remarkably improved the diagnosis of lesions of this area. With the introduction of the contrast medium Gd-DTPA, MR might become even more advantageous. The purpose of this study was to describe our experience with Gd-DTPA in the evaluation of lesions of the nasopharyngeal region.

Materials and Methods

Over a 3-year period 42 patients with primary and secondary tumors of the nasopharynx and adjacent spaces were examined with MR before and after IV injection of the contrast medium Gd-DTPA. Secondary tumors were defined as processes primarily located in adjacent structures but extending into the nasopharynx. The 42 cases comprised 16 primary tumors (11 squamous cell carcinomas, three lymphoepithelial, and two adenoid-cystic carcinomas) and 26 secondary tumors (10 maxillary sinus squamous cell carcinomas, four oropharyngeal tumors, and 12 miscellaneous tumors such as lymphomas, lymphoid hyperplasia, and cysts). The MR findings were compared with the results of contrast-enhanced CT and histologic examinations.

Nine MR examinations were performed at a field strength of 0.35 T and 33 examinations at 1.0 T on a Siemens Magnetom unit. Images were acquired by using a 30-cm head coil. Five- or eight-millimeter-thick sections were made in two or three planes (axial, coronal, sagittal), depending on the extent of the tumor.

Received March 24, 1989; revision requested April 24, 1989; revision received June 2, 1989; accepted June 13, 1989.

[1] Department of Radiology, University of Munich, Marchioninistr. 15, 8000 München 70, West Germany. Address reprint requests to T. Vogl.

[2] Department of Radiology, Neuroradiological Section, Hospital of the University of Pennsylvania, 3400 Spruce St., Philadelphia, PA 19104.

[3] Department of Otorhinolaryngology and Head and Neck Surgery, University of Munich, 8000 München 70, West Germany.

0195-6108/90/1101-0187

TABLE 1: Plain vs Gd-DTPA–Enhanced MR and Gd-DTPA–Enhanced MR vs Contrast-Enhanced CT in the Evaluation of Tumors of the Nasopharynx

Type of Nasopharyngeal Tumor	No.	MR Grade[a]		Gd-DTPA MR vs CT[b]
		Plain	Gd-DTPA	
Primary				
Squamous cell carcinoma	11	2	3	MR+
Lymphoepithelial and adenoid-cystic carcinoma	5	2	3	MR+
Secondary				
Squamous cell carcinoma of maxillary sinus	10	2	2	MR = CT
Tumor of the oropharynx	4	2	3	MR+
Other (e.g., lymphoma, lymphoid hyperplasia, cyst)	12	2	3	MR+
Total	42			

[a] T1-weighted MR, 500/25, was graded on a scale of 0–3. 0 = unsatisfactory; 1 = satisfactory; 2 = good; 3 = optimal. Gd-DTPA was injected in a dose of 0.2 ml or 0.1 mmol/l per kg body weight.

[b] MR+ = MR superior to CT; MR = CT means MR and CT were of equal value.

After a sagittal survey image was obtained for the purpose of craniocaudal orientation, images were obtained in the axial orientation with a long, 1600/25,90 (TR/TE), and a short, 500/25, spin-echo (SE) sequence and in the coronal orientation with a short sequence with the same parameters. After injection of contrast medium, images were obtained in the axial plane with a short SE sequence; 28 cases were also studied in the coronal plane. In seven cases during and after injection of Gd-DTPA, a very short sequence, 30/13, with a flip angle of 30° was performed every minute over a period of at least 8 min in order to measure the change in signal intensity over time. Gd-DTPA was administered in a dose of 0.2 ml or 0.1 mmol/l per kg body weight.

CT scans were obtained on a Siemens Somatom 2 or DRH unit. Four-millimeter-thick sections were obtained after injection of contrast material.

The results of nonenhanced MR, MR with Gd-DTPA, and contrast-enhanced CT were evaluated subjectively. The diagnostically important structures of the nasopharynx were analyzed on T1-weighted (plain and Gd-DTPA), T2-weighted, and proton-density images. The studies were assessed in three separate categories. The first and second categories dealt with the quality of MR images; grades ranging from unsatisfactory (grade 0) to optimal (grade 3) were assigned (Table 1). Grade 0 was defined as unsatisfactory because of motion or metallic artifacts. Grade 1 was defined as allowing recognition of tumor masses at least 5 mm in diameter. Designation of grade 2 meant clear delineation of tumor masses from the most important surrounding structures (such as pterygoid muscles). Studies were given a grade of 3 if, in addition to demarcation of masses, it was possible to identify the smaller anatomic structures (tensor and levator veli palatini muscles), appreciate their relationship to the tumor, and also characterize the tumor tissue (i.e., necrosis, vascularity). The same grading system was used for comparing the value of different pulse sequences (Table 2). In the third category, MR and CT were compared (Table 1).

The actual T1 and T2 relaxation times were determined with the help of the software program of the MR imager. For T1 evaluation two pulse sequences were necessary with different TRs and the same TE; for T2 evaluation a sequence with two echoes was needed. With the scanner operating at 1.0 T, moderate T1 relaxation times were defined as those within a range between 800 and 1300 msec moderate T2 relaxation times as those within a range between 50 and 100 msec. Values below these ranges were defined as low and values above these ranges as high relaxation times. The ratio of signal intensities before and after administration of Gd-DTPA was measured by dividing the signal intensity of the enhanced tumor by the signal intensity of the nonenhanced tumor. A low enhancement factor was defined as one with a ratio of 1.3 or lower. Between 1.3 and 1.8 the enhancement factor was considered medium; above 1.8 the enhancement factor was considered high.

TABLE 2: Comparison of Different MR Pulse Sequences and Gd-DTPA in Evaluating Tumor Infiltration

Location	Grade by MR Pulse Sequence and with Enhancement			
	T1-Weighted	Proton-Density	T2-Weighted	Gd-DTPA
Superficial structures				
Pharyngeal recess	2	3	2	3
Torus tubarius	2	3	2	3
Muscles				
Levator veli palatini muscle	2	2	1	3
Tensor veli palatini muscle	2	2	1	3
Medial/lateral pterygoid muscle	2	3	2	3
Longus colli muscle	2	3	2	3
Deep structures				
Parapharyngeal space	2	3	2	3
Infratemporal fossa	2	2	2	3
Sphenoid bone, skull base	2	2	2	2
Carotid artery	2	2	2	3
Cavernous sinus	2	2	2	3
Eustachian tube	1	2	1	2
Pharyngobasilar fascia	1	1	1	2
Walls of maxillary sinuses	1	2	1	2

Note.—Visualization was graded on a 0–3 scale: 0 = unsatisfactory; 1 = satisfactory; 2 = good; 3 = optimal. MR pulse sequences: T1-weighted, 500/25; proton-density, 1600/25; T2-weighted, 1600/90. Gd-DTPA was administered in a dose of 0.2 ml or 0.1 mmol/l per kg body weight.

Results

The diagnostically important structures of the nasopharynx were analyzed on T1-weighted (plain and Gd-DTPA), T2-weighted, and proton-density images. The normal superficial

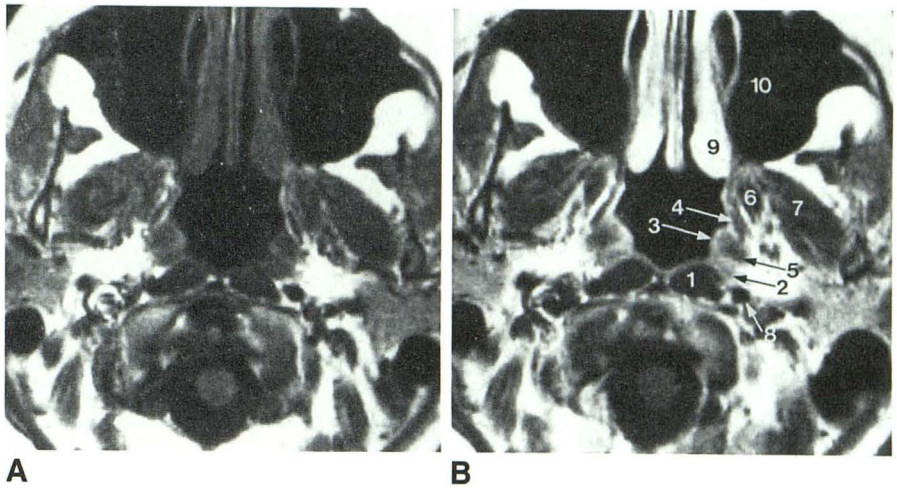

Fig. 1.—Normal anatomy of nasopharyngeal structures on axial MR images, 500/17, before and after Gd-DTPA administration.

A, Plain image. Differentiation of specific nasopharyngeal structures is difficult.

B, After Gd-DTPA enhancement. Enhancement of mucosa, fat, and muscle fasciae provides better anatomic detail. 1 = longus colli muscle; 2 = pharyngeal recess; 3 = torus tubarius; 4 = levator veli palatini muscle; 5 = tensor veli palatini muscle; 6 = medial pterygoid muscle; 7 = lateral pterygoid muscle; 8 = carotid artery; 9 = nasal turbinate; 10 = maxillary sinus.

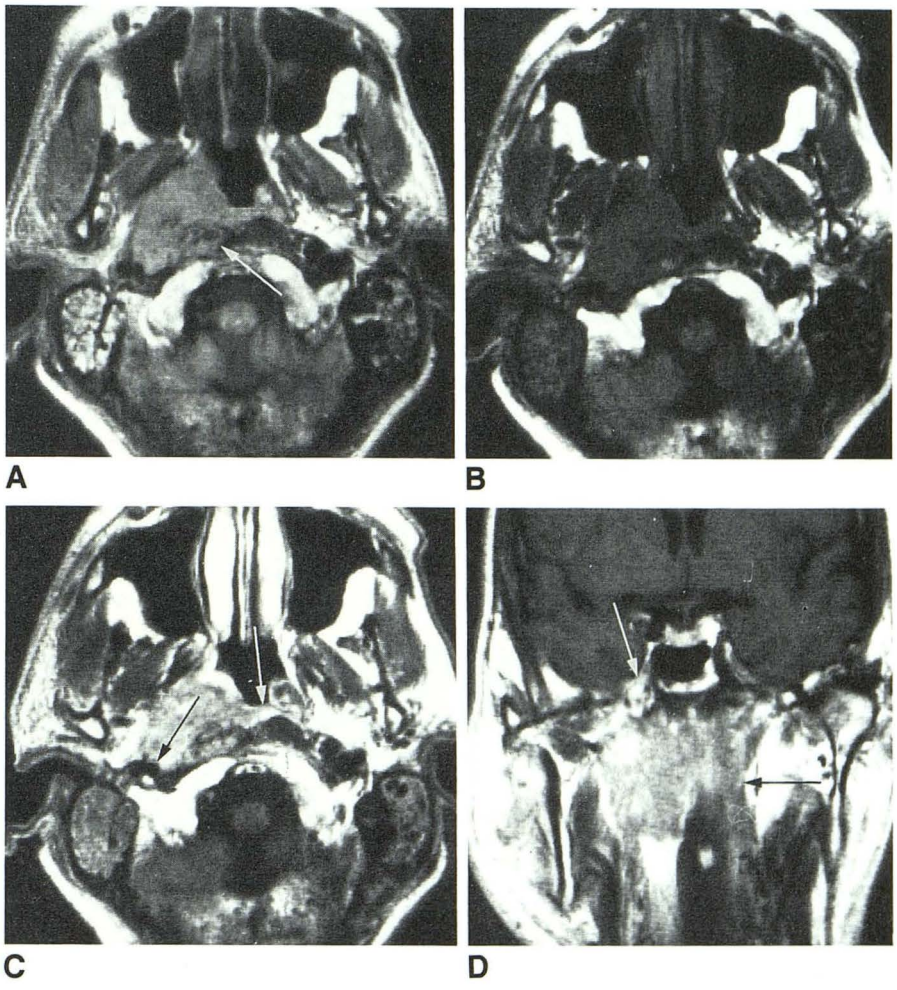

Fig. 2.—Primary squamous cell carcinoma of the nasopharynx.

A, Axial SE 1600/25 image, unenhanced. Right nasopharyngeal tumor of moderate signal intensity infiltrates parapharyngeal space and longus colli muscle (*arrow*). There is destruction of anteroinferior portion of right temporal bone and fluid in mastoid cells.

B, Axial SE 500/25 image, unenhanced. Tumor is of same signal intensity as muscle. It can only be speculated whether or not tumor crosses midline.

C, Axial SE 500/25 image, Gd-DTPA–enhanced. Tumor enhances inhomogeneously and less than mucosa. There is infiltration and displacement of sheath of right carotid artery (*black arrow*), longus colli muscle, torus tubarius, levator and tensor veli palatini muscles, and pharyngobasilar fascia. There is also extension of tumor to right parapharyngeal space with displacement of pterygoid muscle. Midline has been crossed (*white arrow*), and there is infiltration of left pharyngeal recess.

D, Coronal SE 500/25 image, Gd-DTPA–enhanced. Inhomogeneous tumor infiltrates and destroys wall of right sphenoid sinus, infiltrates cavernous sinus (*white arrow*), and crosses midline (*black arrow*).

structures like the torus tubarius and the pharyngeal recess were best delineated on proton-density and Gd-DTPA–enhanced T1-weighted images. The levator and tensor veli palatini muscles, the pterygoid muscles, and the pharyngobasilar fascia were better identified after Gd-DTPA because sharper contrast was achieved between these structures and adjacent tissues. This was due to a slight increase in signal intensity after Gd-DTPA of the normal lymphoepithelial mucosa as well as of fascial planes that surround the muscles (Fig. 1 and Table 2). Arteries usually show a flow void, but at

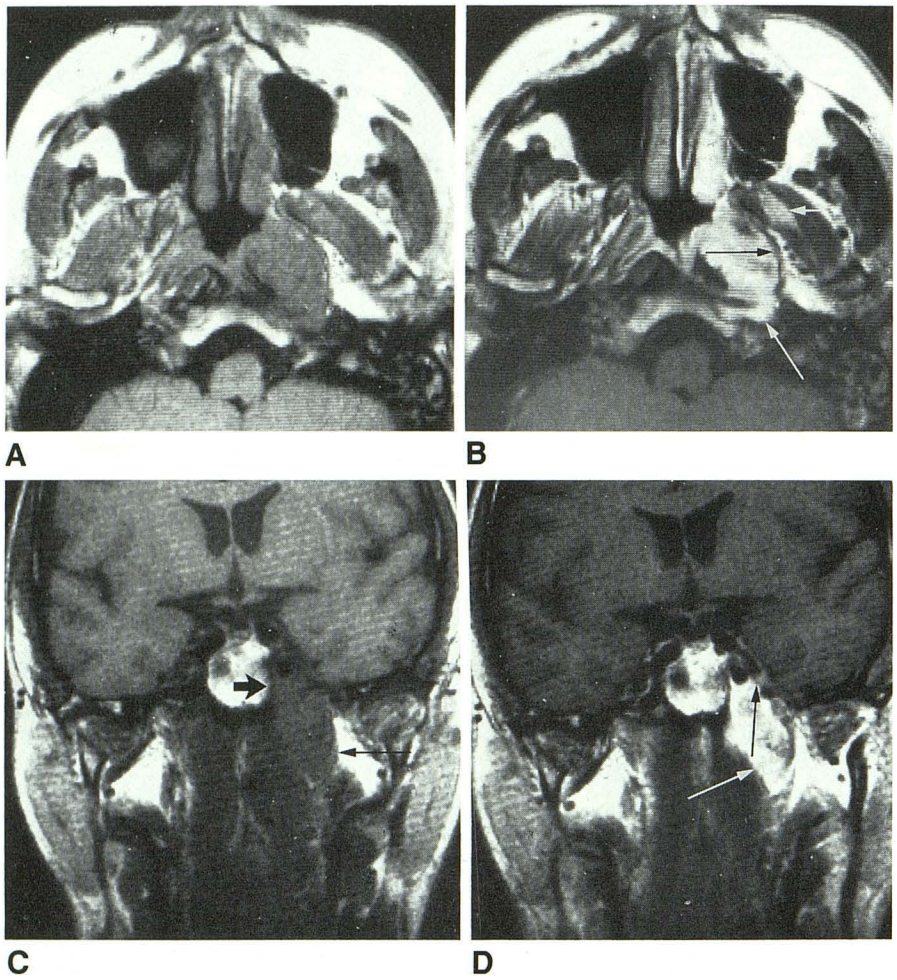

Fig. 3.—Adenoid-cystic carcinoma of nasopharynx.

***A*, Axial SE 500/25 image, unenhanced. Exact delineation of left nasopharyngeal tumor is not possible because it has the same signal intensity as muscles and mucosa.**

***B*, Axial SE 500/25 image, Gd-DTPA–enhanced. There is marked enhancement of tumor, which destroys skull base (*long white arrow*) and infiltrates levator veli palatini and longus colli muscles on left side. There is also infiltration of left pterygoid muscles (*short white arrow*). Differentiation of tumor from enhanced left turbinate is difficult. Left margin of tumor is well demarcated by muscles it has displaced, thus indicating expansion and not infiltration of parapharyngeal space (*black arrow*).**

***C*, Coronal SE 500/25 image, unenhanced. There is good delineation of tumor from fat (*long arrow*), but not from adjacent muscles. There is destruction of cranial base with extension into clivus (*short arrow*).**

***D*, Coronal SE 500/25 image, Gd-DTPA–enhanced. Skull-base infiltration and involvement of cavernous sinus (*black arrow*) are seen better after tumor enhancement. Also, enhancement provides a sharp interface between tumor and longus colli muscle (*white arrow*). However, tumor and fat are of similar intensities.**

TABLE 3: Characterization of Common Tumors of the Nasopharynx

Type of Tumor	Tumor Extent	Margins	Homogeneity	Signal Intensity	Enhancement Factor
Primary squamous cell carcinoma	Nasopharyngeal mucosa, nasal cavity, infiltration of skull base	Unsharp	Necrotic areas, inhomogeneous	Moderate T1, moderate T2	1.6
Lymphoepithelial and adenoid-cystic carcinomas	Aggressive growth with skull-base infiltration	Sharp	Some necrosis	Moderate T1, moderate to high T2	2.0
Secondary squamous cell carcinomas	Infiltration and destruction of maxillary sinuses	Unsharp	Necrosis, inhomogeneous	Low to moderate T1, moderate T2	1.8
Lymphoma	Rarely, bony infiltration	Sharp	Homogeneous	Moderate T1, moderate T2	1.6

Note.—Enhancement factor is a ratio of signal intensities before and after Gd-DTPA. Moderate T1 values were 800–1300 msec; moderate T2 values were 50–100 msec. Values below these ranges were defined as low and values above these ranges as high relaxation times. Pulse sequences: T1-weighted, 500/25; T2-weighted, 1600/90; proton-density, 1600/25.

the skull base veins with slowly flowing blood can be identified before and after Gd-DTPA as structures of high signal intensity. For demonstrating bony structures of the skull base, such as the clivus, the value of the contrast-medium–enhanced T1-weighted sequence depends on the increase in the signal intensity of the tumor. If the tumor showed a great increase it was sometimes difficult to delineate it from fat and bone marrow, which also enhanced prominently. In the case of minimally or moderately enhancing tumors, the bone marrow after Gd-DTPA was brighter than the tumor, and infiltration of the tumor into bony structures was seen very well. The nasal mucosa and turbinates often get very bright on

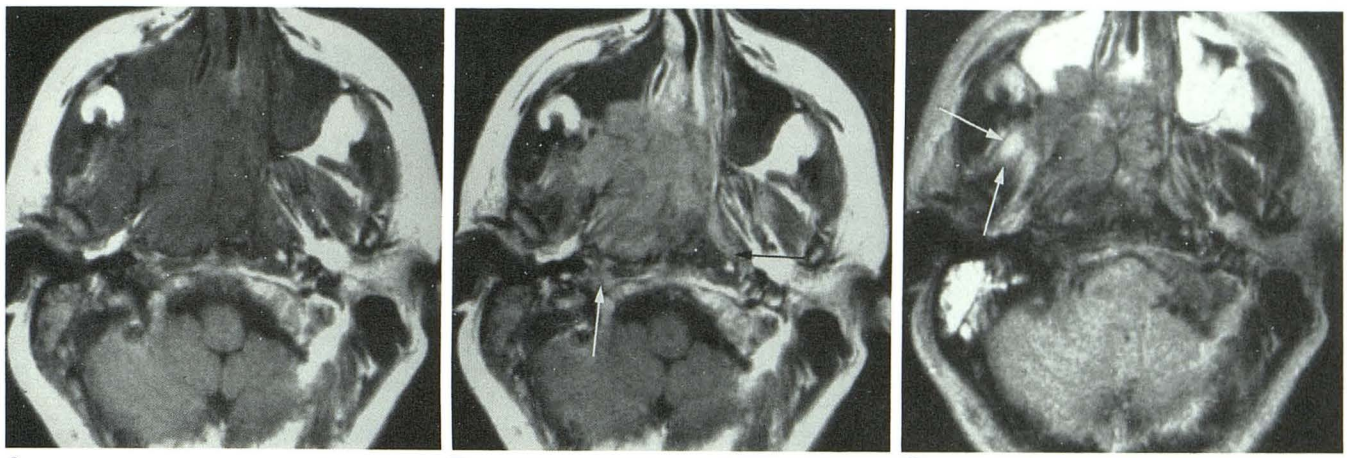

Fig. 4.—Maxillary sinus carcinoma involving nasopharynx.

***A*, Axial SE 500/25 image, unenhanced. Large tumor has produced destruction of posterior wall of right maxillary sinus and has infiltrated nasopharynx, parapharyngeal space, and infratemporal fossa. Right pterygoid muscle appears infiltrated by tumor. Tumor shows low signal intensity and homogeneous pattern.**

***B*, Axial 500/25 image, Gd-DTPA–enhanced. After administration of Gd-DTPA, tumor shows an increase in signal intensity in comparison with fluid in maxillary sinuses. Intact enhanced mucosa is identified in anterior part of nasal cavity. Tumor has destroyed posterior part of right maxillary sinus, posterior part of nasal cavity, and inferior aspect of temporal bone (*white arrow*) and has infiltrated prevertebral muscles. Middle third of right lateral pterygoid muscle does not enhance as much as tumor (compare with *C*). Left parapharyngeal space and left pharyngeal recess appear uninvolved (*black arrow*).**

***C*, Axial SE 1600/90 image, unenhanced. T2-weighted image allows good differentiation between tumor tissue and hyperintense fluid in maxillary sinus. Middle third of right pterygoid muscle is of high signal intensity (*arrows*), thought to represent edema at edge of tumor. Fluid is in mastoid sinus.**

enhanced MR. Therefore, it may be difficult to completely delineate an enhancing tumor if it is contiguous with the nasal cavity.

In 16 patients with primary nasopharyngeal tumors 11 patients had squamous cell carcinomas. All these tumors showed an infiltration of the levator and tensor veli palatini muscles and of the pharyngobasilar fascia. Because of eustachian tube obstruction, fluid was seen in the mastoid cells in 10 of these patients. Seven squamous cell carcinomas invaded the sphenoid and cavernous sinuses and three extended to the nasal cavity. Unsharp margins and necrotic areas were characteristic of these tumors (Fig. 2). Low-intensity nonenhancing regions within the tumor mass were considered to represent necrosis; this was confirmed at surgery. A discrete crossing of the midline by the tumor could be seen only on the contrast-enhanced images, but was suspected on the preenhancement images (Fig. 2). Gross infiltration of the longus colli muscle was well demonstrated on enhanced MR but was also well shown on the proton-density images. However, subtle extension of these tumors to the pterygoid muscles could be judged best on images with Gd-DTPA enhancement, because the signal intensity of squamous cell carcinomas on the plain image was about the same as that of muscles. The squamous cell carcinomas

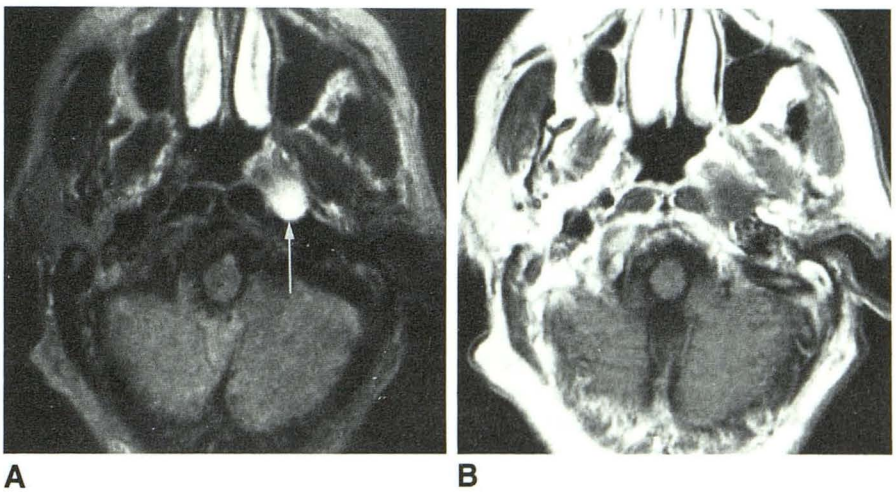

Fig. 5.—Cyst of naso- and oropharynx (surgically proved).

***A*, Axial SE 1600/90 image, unenhanced. Sharply delineated lesion of high signal intensity (*arrow*) is located in left nasopharynx.**

***B*, Axial SE 500/25 image, Gd-DTPA–enhanced. There is no enhancement of cyst, which displaces normal nasopharyngeal structures anteromedially. A lower section (not shown) demonstrated contrast enhancement of cyst wall.**

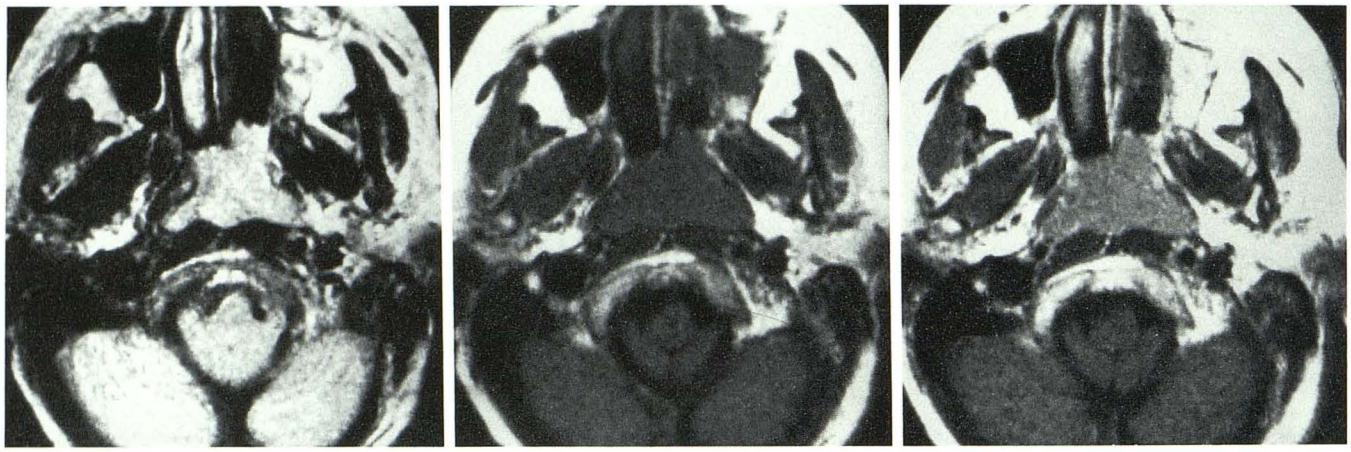

Fig. 6.—Lymphoma of nasopharynx.
***A*, Axial SE 1600/90 image, unenhanced. Nasopharynx is completely filled with homogeneous tissue. Proton-density image (not shown) showed slightly higher signal intensity in mass when compared with signal intensity of muscles. Fluid is in left maxillary sinus.**
***B*, Axial SE 500/25 image, unenhanced. Tumor on T1-weighted images has signal intensity similar to that of brain.**
***C*, Axial SE 500/25 image, Gd-DTPA–enhanced. Tumor shows homogeneous pattern of enhancement. There is no infiltration, but slight compression of veli palatini muscles bilaterally.**

showed a medium increase after Gd-DTPA administration. The calculation of relaxation times showed moderate T1 and moderate T2 values. We examined three patients with lymphoepithelial and two patients with adenoid-cystic carcinomas. These tumors showed an aggressive growth pattern with early skull-base infiltration (Fig. 3). In some cases, it was difficult even after Gd-DTPA to judge whether the tumor crossed the midline or not. In our experience, the normal mucosa generally showed a greater increase in signal intensity after administration of Gd-DTPA than tumor masses did. On the contrast-enhanced image these tumors had sharp margins with small necrotic areas. Adenoid cystic and lymphoepithelial carcinomas had a high enhancement factor of about 2, moderate T1, and moderate to high T2 values (Table 3).

The most frequent secondary nasopharyngeal tumors were squamous cell carcinomas of the maxillary sinuses. In 10 patients these tumors showed characteristics similar to the primary nasopharyngeal carcinomas. As in the primary carcinomas, we found a moderate increase in signal intensity after administration of Gd-DTPA and moderate T1 and T2 values. On plain T1-weighted and on proton-density images it was difficult or impossible to differentiate tumor masses in the maxillary sinus from inflammatory changes and fluid. These could be distinguished on enhanced MR, but the distinction was clear on T2-weighted images, on which fluid was very bright and tumor was of low intensity. If the posterior part of the tumor infiltrated the longus colli muscle, it could be judged best on enhanced MR images. Also, discrimination between inflammation and tumor in the anterior part was possible on these images (Fig. 4). Infiltration of the bony walls of the maxillary sinuses was seen better on CT, but the exact extension of the tumor was seen better on MR.

A further advantage of contrast-enhanced MR was the discrimination between solid tumor and fluid-containing cystic processes. In our patient group one patient had a cyst of the nasopharynx and oropharynx (Fig. 5). A solid tumor was excluded and the likelihood of a cystic process was supported after Gd-DTPA.

Another important differential diagnosis, especially in young patients, is the discrimination between lymphoid hyperplasia and any kind of lymphoma. In two patients with lymphoma and in three patients with lymphoid hyperplasia, we saw no difference in the tumor pattern on T1-weighted plain images and T2-weighted images. Only small asymmetry was noted in the nasopharyngeal mass due to a lymphoma. After injection of the contrast medium Gd-DTPA, the lymphoid hyperplasia showed septations in its internal pattern (Fig. 6). The lymphoma did not enhance as much as lymphoid hyperplasia did and its inner structure was homogeneous (Fig. 7).

The fast imaging technique was used in four cases of primary squamous cell carcinomas, two cases of secondary squamous cell carcinomas, and one case of lymphoepithelial carcinoma. Lymphoepithelial carcinoma reached an optimal increase in signal intensity after 180 sec and squamous cell carcinomas after 240 sec, with a slight decrease after that time. Three examinations were unsatisfactory because of motion or metallic artifacts.

Discussion

With both CT and MR, it is necessary to carry out the examination using at least two orientations, axial and coronal; however, coronal scanning is often difficult to perform in CT, particularly in older patients. In our study, sagittal views did not support the diagnostic management; only two or three midline slices were useful. No additional information was provided over that obtained with axial and coronal slices. CT provides better resolution of cortical bone detail [4–8]. However, even with contrast enhancement, CT delineation of muscles and mucosa from tumor is often unsatisfactory. The

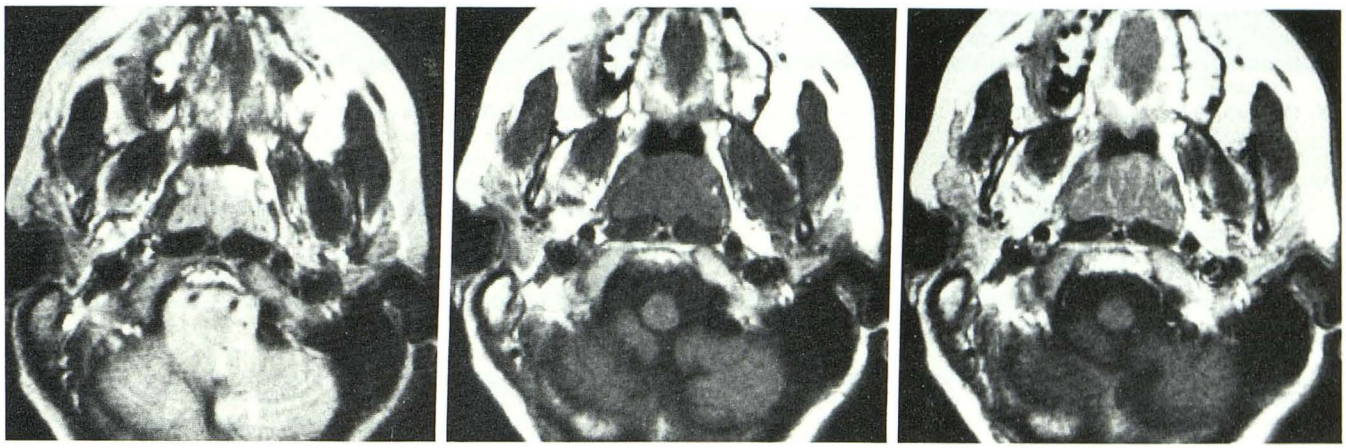

Fig. 7.—Lymphoid hyperplasia in nasopharynx.

***A*, Axial SE 1600/90 image, unenhanced. On T2-weighted image, nasopharyngeal tissue is bright and shows slight inhomogeneity and scattered internal patterns.**

***B*, Axial SE 500/25 image, unenhanced. Mass is sharply marginated, symmetrical, and of homogeneous low signal intensity. It has appearance similar to that of lymphoma in Fig. 6.**

***C*, Axial SE 500/25 image, Gd-DTPA–enhanced. After Gd-DTPA administration, tumor shows moderate increase in signal intensity with inhomogeneous internal pattern mainly consisting of septations. As in lymphoma, there is compression of veli palatini muscles on both sides.**

accurate relationship to vessels and nerves often cannot be demonstrated [9]. With MR, multiplanar imaging can show tumor extension in all three orientations, especially extension along cranial nerves V, VII, IX, and X [10–12]. MR with Gd-DTPA allows recognition of infiltration or involvement of the sheath of the carotid artery and the jugular vein. Also, contrast-medium–enhanced MR, with its better soft-tissue contrast, allows exact differentiation among small anatomic details, such as demonstration of both palatini muscles and the pharyngobasilar fascia [12, 13]. This fascia, as an essential structure for the evaluation of diseases of the nasopharynx, is not seen on CT scans. It separates the two most important compartments, the parapharyngeal space and the intrapharyngeal structures. Infiltration of this fascia is a sure sign of an aggressive tumor [4, 10, 11, 14].

In the differential diagnosis between tumor and inflammation, MR with T1- and T2-weighted sequences is superior to CT. Information regarding inflammation was best seen on T2-weighted images, but discrimination was also possible on contrast-enhanced T1-weighted sequences because the tumor usually did not enhance as much as the inflamed tissues.

Cystic processes with high signal intensities on T2-weighted images show no significant enhancement after contrast medium, but the walls of the cysts do enhance [15]. Contrast-enhanced MR allows appreciation of the internal patterns of the neoplasm, as for example necrosis or vascularity, but with both MR and CT mucosal spreading tumors were difficult to detect because the mucosa shows a high signal intensity on plain MR that increases after injection of Gd-DTPA. If tumor infiltrates bone marrow it is sometimes difficult to distinguish bone marrow from tumor. Both marrow and tumor enhance after administration of Gd-DTPA; the type of tumor determines which one becomes brighter. If the tumor shows an area of hemorrhage at a stage when it is very bright on the T1-weighted nonenhanced image, after Gd-DTPA the tumor will enhance but the hemorrhage will not; thus, it may be difficult to differentiate between solid tumor and hemorrhage after Gd-DTPA administration. There is only limited experience concerning the fast imaging technique with Gd-DTPA for nasopharyngeal tumors. We have yet to find a significant difference; the different patterns of Gd-DTPA enhancement do not enable correlation between findings and histologic features. But different enhancement factors might be a criterion for discrimination.

It appears that Gd-DTPA is helpful in delineating nasopharyngeal tumors and their extension [16], but unenhanced T1 and T2 images are still needed. In addition, CT scans should be obtained if there is any question about infiltration of cortical bone.

The advantages of Gd-DTPA are better delineation of early infiltration by tumors and the possibility of improving differential diagnostic considerations. In diagnosing diseases of the nasopharynx and surrounding tissues, MR with Gd-DTPA is recommended as the method of choice in the evaluation of small tumors with infiltrating growth patterns, which are difficult to detect on the initial nonenhanced MR examination. Gd-DTPA is not needed in tumors that are well demarcated on plain T1- and T2-weighted sequences. In the follow-up to determine tumor recurrence, contrast medium is helpful when visualization of tumor areas is poor on T1- and T2-weighted nonenhanced images. The improved tumor delineation and identification of spread are helpful in planning radiation therapy.

REFERENCES

1. Dillon WP, Mills CM, Kjos B, Degroot J, Brant-Zawadzki M. Magnetic resonance imaging of the nasopharynx. *Radiology* **1984**;152:731–738

2. Lloyd G, Land V, Phelps P, Howard D. MRI in evaluation of nose and paranasal sinus disease. *Br J Radiol* **1987**;60:957–968
3. Mödder U, Lenz M, Steinbrich W. MRI of facial skeleton and parapharyngeal space. *Eur J Radiol* **1987**;7:6–10
4. Mancuso AA, Hanafee WN. Nasopharynx and parapharyngeal space. In: *Computed tomography and magnetic resonance imaging of head and neck*. Baltimore: Williams & Wilkins, **1985**:428–443
5. Zinreich SJ, Kennedy DW, Rosenbaum AE, Gayler BW, Kumar AJ, Stammberger W. Paranasal sinuses: CT imaging requirements for endoscopic surgery. *Radiology* **1987**;163:769–775
6. Bohman RN, Mancuso AA, Thompson J, Hanafee W. CT approach to benign nasopharyngeal masses. *AJR* **1981**;136:173–180
7. Silver JA, Mawad ME, Hilal SK, et al. Computed tomography of the nasopharynx and related spaces. Part I: Anatomy. *Radiology* **1983**; 147:725–731
8. Silver JA, Mawad ME, Hilal SK, et al. Computed tomography of the nasopharynx and related spaces. Part II: Pathology. *Radiology* **1983**; 147:733–738
9. Hagemann J, Witt CP, Jend-Rossmann T, Hörmann L, Jend HH, Bücheler E. Wertigkeit der Computerromographie bei Tumoren des Epi- und Oropharynx. *ROFO* **1983**;139:373–378
10. Teresi LM, Lufkin RB, Hanafee WN, et al. MR imaging of the nasopharynx and floor of the middle cranial fossa. Part I: Normal anatomy. *Radiology* **1987**;164:811–816
11. Teresi LM, Lufkin RB, Hanafee WN, et al. MR imaging of the nasopharynx and floor of the middle cranial fossa. Part II: Malignant tumors. *Radiology* **1987**;164:817–821
12. Vogl T. Kernspintomographie des Gesichtsschädels. In: Lissner J, Seiderer M, eds. *Klinische Kernspintomographie*. Stuttgart: Enke, **1986**:210–220
13. Mees K, Vogl T, Bauer M. MRI in diseases of head and neck—diagnostic possibilities. *Laryngo Rhinol-Otol* (Stuttg) **1987**;66:543–546
14. Mancuso AA, Bohman L, Hanafee W, Maxwell D. Computed tomography of the nasopharynx: normal and variants of normal. *Radiology* **1980**; 137:113–121
15. Römer T, Tausch-Treml R, Hamm B, Felix R, Wolf K-J. KST der Nasennebenhöhlen unter Verwendung von Gd-DTPA and Multiecho-Sequenzen. *ROFO* **1988**;149:171–177
16. Vogl T, Brüning R, Grevers G, Mees K, Bauer M, Lissner J. MRI of the oropharynx and tongue: comparison of plain and Gd-DTPA studies. *J Comput Assist Tomogr* **1988**;12:3–12